

Landscape and Pedogenesis of an Oxisol–Inceptisol–Ultisol Sequence in Southeastern Brazil

L. H. Anjos,* M. R. Fernandes, M. G. Pereira, and D. P. Franzmeier

ABSTRACT

The topographic sequence of Oxisols, Inceptisols, and Ultisols is frequently observed in tropical hilly surfaces in the southeastern region of Brazil. The purpose of this study was to relate pedogenesis to major geomorphic surfaces (MGS) in the Caetés watershed, located in Paty do Alferes, Rio de Janeiro State. The landscape is characterized by steep bedrock hills and cliffs of pre-Paleozoic gneiss, granite, and related metamorphic rocks rising above long, nearly level, accordant ridge crests, convex hills, and narrow fluvial plains. Intense soil development, with deep weathering and kaolinite formation in the gneiss–granite rock, took place on the ridges and convex hills. Six pedons were examined using field investigation and laboratory soil characterization techniques. The degree of pedogenesis on the various geomorphic surfaces supports the landscape evolution theories of Penck and King. A Typic Hapludox, with the greatest degree of pedogenesis, formed on the stable summit position, MGS1. The upper part of the retreating slope, MGS2, bevels MGS1, and the material eroded from MGS2 moved downslope and formed a surface with lower gradient, MGS3. Dystrochrepts are on shoulder positions and shallow Hapludox are on backslope positions of the geomorphic surface MGS2, and Kandiuults formed on footslopes, MGS3. Eutrochrepts are on the youngest surface MGS4, a toeslope position.

SEVERAL THEORIES have been developed to explain the evolution of landscapes under varying conditions of climate. The Davisian system of slope decline is commonly applied to explain landscape development in humid climates (Davis, 1899, as cited by Carson and Kirkby, 1972, p. 11–12 and 369–377, and Daniels and Hammer, 1992, p. 145–146). According to Davis' concepts, after the rapid uplift of a landmass and stream incision, denudation processes result in the lowering of the landscape, with the progressive decrease of the slope gradient of the valley sides. The result is the formation of a *peneplain*, a very gently sloping surface. In this model, the divide surface lowers constantly, thus relict landscapes do not exist and the whole landscape is of about the same age.

In Penck's model of slope replacement (Penck, 1953, as cited by Carson and Kirkby, 1972, p. 13–17 and 372–377, and Daniels and Hammer, 1992, p. 146), the development of side slopes occurs in a succession of erosional intensity and denudation where specific contours and gradients are produced. A slope of lesser gradient replaces one of greater gradient. As a result, several geomorphic surfaces of different ages, including relict landscapes, can occur within one landscape.

In arid or semiarid regions, the model of parallel

slope retreat or backwearing, attributed to L.C. King (Bigarella et al., 1965a), is usually applied to explain the succession of high-level erosion surfaces separated from each other by steep scarps. In this model, denudation of the landmass takes place through parallel retreat of the slope walls, resulting in the emergence of basal pediments, which eventually coalesce to form wide *pediplains*. The typical slope profile has an upper waxing slope followed downslope by a free face, which has the greatest gradient, a debris slope, and a pediment at the valley floor.

According to Bigarella et al. (1965a,b), Davis' theory could not thoroughly explain the genesis of the tropical hilly surfaces in the southeastern region of Brazil. They postulated pedimentation processes and climate-induced episodic erosion–sedimentation cycles, caused by great cyclic climatic changes in the Serra do Mar region during the Cenozoic, to account for the origin of these hillslopes.

A cratonic shield forms the mountainous range along the Brazilian southeastern coastal region. It consists mainly of Pre-cambrian rocks that, since the Silurian, have been tectonically undisturbed except for local reactivation of the main fault lines (Salamuni and Bigarella, 1967).

The region of Paty do Alferes represents many mountainous areas of Rio de Janeiro and other states in southeastern Brazil. The landscape is characterized by steep bedrock hills and cliffs of gneiss, granite, and related metamorphic rocks, rising above long, nearly level, accordant ridge crests, deeply weathered convex hills (called *meias laranjas*—half oranges), and narrow fluvial plains (Departamento de Recursos Minerais, 1995). The accordant ridge crests are considered to be remnants of an old erosional surface, dating back to the Early Cretaceous, which was renewed after the Serra do Mar uplifting (Departamento de Recursos Minerais, 1995). The shoulder, mid-, and footslopes are apparently the results of incision during post-Early Cretaceous erosion cycles that were responsible for the general lowering and undulating nature of the landscape. Other events (during the Quaternary) included several phases of colluviation of gneiss–granite regolith, deposition of materials in concave footslope sites, and limited filling of valley bottoms by alluvium. The distribution of soils is apparently related to the sequence of geomorphic surfaces observed at the Caetés watershed and in other basins within the Paty do Alferes region (EMBRAPA–Centro Nacional de Pesquisa de Solos, 1996, not published).

L.H. Anjos, M.R. Fernandes, and M.G. Pereira, Soils Dep., UFRRJ, Seropédica, RJ, Brazil 23890-000; D.P. Franzmeier, Agronomy Dep., Purdue Univ., West Lafayette, IN 47907. Purdue Univ. Agric. Res. Programs Journal Paper no. 15497. Supported in part by CAPES/CNPQ program, Brazil, and EMBRAPA/CNPS-CEE. Received 11 Aug. 1997. *Corresponding author (lanjos@ufrrj.br).

Abbreviations: CBD, citrate–bicarbonate–dithionite solution; CEC, cation-exchange capacity; ECEC, effective cation-exchange capacity; Fe_d, Fe extracted with CBD.; Fe_o, Fe extracted with oxalate solution; GS, geomorphic surfaces; MGS, major geomorphic surfaces; Si, Al, and Fe, Si, Al, and Fe extracted with H₂SO₄, respectively.

Variations of topography are indicative of changes in solum depth and degree of chemical weathering. According to Alexander (1995), surface wash and solution loss are generally the dominant processes on moderately steep slopes. Solution loss predominates where weathering produces regolith or soil faster than it is removed by particulate erosion, and surface wash prevails where water carries away soil so rapidly that soil or regolith does not accumulate to produce deep sola. Alexander (1995) found fewer shallow soils on moderately steep (15–30%) than on steep (31–70%) slopes in humid northwestern California. Differences in soil color down-slope have been observed and described by many researchers. In hilly tropical soil landscapes, a sequence of red to red-yellow and yellow to gray soils, from well-drained hilltops to poorly drained valleys, is the most frequent pattern. This sequence is commonly related to increasing wetness conditions (Moniz and Buol, 1982, and Curi and Franzmeier, 1984, in Brazil; Munnik et al., 1992, in South Africa; Peterschmitt et al., 1996, in South India).

The purpose of this study was to relate observed pedogenesis to geomorphic surfaces in the Caetés watershed, located in Paty do Alferes, Rio de Janeiro. The specific objective was to assess the influence of parent material stratigraphy and geomorphic surfaces on the degree of pedogenesis.

MATERIALS AND METHODS

Site Location and Characteristics of Soils

The Caetés agricultural watershed (Fig. 1) is located in Paty do Alferes municipality, latitude of 22°23'42" to 22°24'40"S and longitude of 43°26'00" to 43° 8'22"W. The watershed area

is approximately 1.9 km². Elevation in the watershed ranges from 760 to 780 m along the divide, to approximately 600 m at the valley floor. The climate has warm wet summers and mild dry winters. The mean summer air temperature is 24°C, and the mean winter air temperature is 17°C. The total annual precipitation is about 1250 mm, most of which occurs in the summer, between October and April. The well-drained soils have a udic soil moisture regime and an isothermic soil temperature regime (Van Wambeke, 1981). The natural vegetation is semideciduous tropical broadleaf Atlantic forest. From the preliminary survey of the area, four MGS were identified in the Caetés watershed and six sites were selected along a toposequence (Fig. 1 and 2, Table 1). Profile P1, formed from the clay weathered mantle on the summit position, represents MGS1. Surface MGS2 is represented by Profiles P2, P3, and P4 formed in weathered biotite gneiss, with P2 on the upper shoulder, P3 on the lower shoulder, and P4 on the backslope. Profile P4 also shows contribution of colluvium sediments derived from the gneiss rock. Profile P5 formed in clayey colluvium on the footslope, MGS3, and P6 formed in sandy loam to loamy fluvial deposits on the flood plain of MGS4. The relief varies from moderately steep slope gradients (20–35%), to gently sloping (5–15%) footslopes, and nearly level slopes (1–2%) on the flat summit and basin fill. Sites on the ridge top and slopes are somewhat excessively drained or well drained. On the valley floor, the drainage classes of dominant soils are moderately well drained, with few areas of somewhat poorly drained soils.

Soil Description and Laboratory Analyses

Pedons were described (Table 2) and sampled according to the methods of Soil Survey Staff (1993). Bulk density cores were collected from horizons downward to 1.5 m. The lower limit of observation was the common occurrence of weatherable primary minerals usually in the BC or C horizon, or a depth of 2 m. Supplementary samples were collected with an

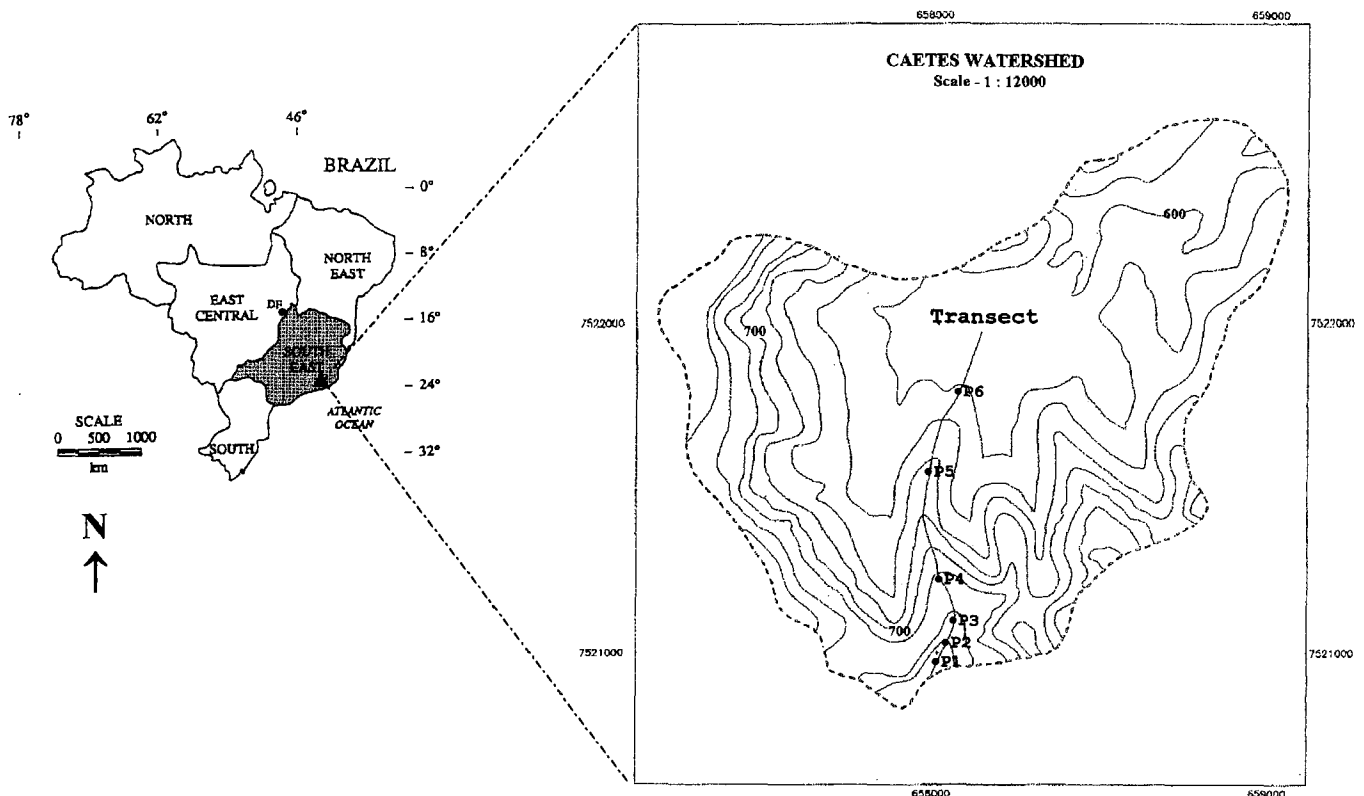


Fig. 1. Diagram of southeastern Brazil, Caetés watershed, and transect studied. Contours are in meters above sea level.

auger on the MGS1 surface to 4-m depth. Bulk soil samples were air dried, crushed with a wooden rolling pin, passed through a 2-mm sieve, and reserved for subsequent analysis following standard soil survey characterization procedures, as described in EMBRAPA/SNLCS (1979).

Particle-size distribution was determined by the pipette method, after dispersion of soil by adjusting the pH to 10 to 11 with 1 M NaOH, and sand sieving. Bulk density was calculated from the weight of the oven-dry mass and volume of the soil core. For chemical analyses, samples of the fine earth fraction (soil <2 mm) were extracted with 1 M KCl for Ca^{2+} , Mg^{2+} , and Al^{3+} , with 0.05 M HCl and 0.025 M H_2SO_4 for K^+ and Na^+ , and with pH 7.0 1 M $\text{Ca}(\text{OAc})_2$ for extractable acidity ($\text{H}^+ + \text{Al}^{3+}$). Extractable H^+ was calculated by subtracting the titrated Al from extractable acidity. Cation-exchange capacity (CEC) was calculated from the sum of base cations (Ca^{2+} , Mg^{2+} , K^+ , and Na^+) plus extractable acidity. The CEC of the total clay fraction was calculated from the CEC for the whole soil, the clay content, and an allowance for the CEC of organic matter [$\text{CEC}/\text{clay} = (\text{CEC sum}) - (4.5 \times \% \text{Corg})/100/\% \text{clay}$], according to EMBRAPA/SNLCS (1988) procedures but in variance with USDA practices (Soil Survey Staff, 1996). Total C was determined by wet oxidation with $\text{K}_2\text{Cr}_2\text{O}_7$. As an estimate of chemical composition of minerals in the clay fraction, the samples were extracted with strong 9 M H_2SO_4 for 1 h, and Si, Al, and Fe in the extract were determined. Citrate-bicarbonate-dithionite (Mehra and Jackson, 1960) and ammonium oxalate (in the dark) extraction procedures (Schwertmann, 1964) were also applied. The content of Si was determined by colorimetric methods, and Fe and Al by absorption spectroscopy.

Minerals in the sand fractions were identified by optical microscopy (Winchell and Winchell, 1951). The clay fraction (<2 μm) was separated using methods described by Jackson (1969), and analyzed by x-ray diffraction of oriented mounts with the following treatments: K saturated at 25°C, and heated to 300°C; Mg saturated; and Mg-glycerol saturated. The samples were step scanned from 2 to 36° 2 θ using 0.02° steps and 1-s count times on a Rigaku D-Max IIA diffractometer (CuK α , $\lambda = 0.154050$ nm, 20 kV, 30 mA).

RESULTS AND DISCUSSION

Morphology, Classification, and Pedon Properties

Soil Morphology and Physical and Chemical Properties

The Bo horizons of Oxisols observed on ridgetops of the Caetés watershed (P1), MGS1, have a $\text{SiO}_2/\text{Al}_2\text{O}_3$ molar ratio of ≈ 1.67 , low total Fe content (39.2–46.9 g

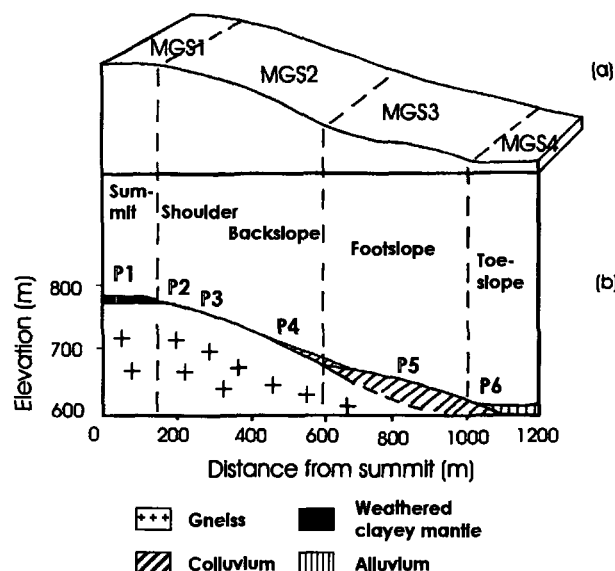


Fig. 2. Relationship between (a) major geomorphic surfaces (MGS) and (b) soils in the Caetés watershed, and the concept of catena (a) proposed by Milne (1936) with the designations according to Ruhe (1960).

kg^{-1} , Fe), and a predominance of goethite in the clay fraction, as indicated by the yellowish colors in Bo1 and Bo2 horizons (10YR hue, 4–5 value, and 4–6 chroma) and the x-ray diffraction data. Samples taken at 3- to 4-m depth, however, showed greater value and chroma, indicating differences in the Fe content or its oxidation or crystallization, when compared with the colors observed in the upper part of the soil profile. The other soils along the transect have redder hues and shallower profiles, with stronger influences of the gneiss parent material. Profile P1 also shows lower values of CEC and effective CEC (ECEC) of the clay fraction (Table 3), Fe_d/Fe_t , Fe_o/Fe_d , and Fe_d/clay ratios (0.46, <0.01, and 0.033, respectively) than Profiles P2 to P6, which developed more recently and from the gneiss regolith or colluvial and alluvial sediments.

On the shoulder position of MGS2, Inceptisols developed from gneiss regolith (P2 and P3) show 10R and 2.5YR hues, and clay CEC of 7.5 and 11.9 $\text{cmol}_c \text{kg}^{-1}$, respectively, in the Bw horizons, and no prevalence of an illuviation process. The continuity between the solum and saprolite, and the absence of stone lines or abrupt

Table 1. Geomorphic surfaces, landscape features, and classification of soils studied.

Site pedon	Landform	Slope	Soil taxonomy†	Brazilian classification subgroup‡
		%		
MGS1	Summit			
P1	Broad upland flat, ridge	2	Fine, kaolinitic Typic Hapludox	Dystrophic, clayey texture, Yellow Latosol
MGS2	Retreating slope			
P2	Nose slope, shoulder	20	Fine-loamy, siliceous, subactive Umbric Dystrochrept	Dystrophic, medium texture, Cambisol
P3	Nose slope, shoulder	20	Fine, kaolinitic Umbric Dystrochrept	Allic, clayey texture, Cambisol
P4	Nose slope, backslope	25	Very fine, kaolinitic Typic Hapludox§	Allic, clayey texture, Yellow-red Latosol
MGS3	Replacement slope			
P5	Footslope	15	Fine, kaolinitic Typic Kandiodult§¶	Dystrophic, medium over clayey texture, Yellow-red Podzolic soil
MGS4	Alluvial fill			
P6	Toeslope	1	Fine loamy, siliceous, subactive Dystric Eutrochrept	Eutrophic, medium texture, Cambisol

† Soil Survey Staff (1996). Soils are all in the isothermic family.

‡ EMBRAPA/SNLCS (1988). Soils are in the moderate A, low activity clay (Tb) class.

§ After micromorphological analysis of thin sections, in order to identify illuviation cutans.

¶ Typic Paleudult subgroup, if the carbon CEC is not subtracted in the calculation of clay CEC in the Bt1 horizon.

Table 2. Morphological properties of the soils (Soil Survey Staff, 1993).

Profile	Depth cm	Horizon	Moist color	Texture†	Structure‡			Consistence§		Boundary width
					Gr	Cl	Sh	Ad	Fc	
P1	0-6	Ap	10YR 2/2	SC	S	F	Gr	SH	FR	Gradual
	6-17	AB	10YR 3/2	C	S	F	Sbk	SH	FR	Gradual
	17-39	BA	10YR 4.5/4	C	M	VF,F	Sbk	SH	FR	Diffuse
	39-100	Bo1	10YR 5/4	C	M	VF,F	Sbk	SH	VFR	Diffuse
	100-141	Bo2	10YR 5/6	C	M	F	Sbk	SH	VFR	Diffuse
	141-200+	Bo3	5YR 5/4	C	-	-	-	-	-	-
P2	0-16	A	10R 3/2	SC	M	F,M	Gr	H	VFR	Clear
	16-50	Bw	10R 4/4	SCL	M	F	Sbk	SH	VFR	Gradual
	50-160+	BC	10R 4/3	SL	W	F	Sbk	SH	VFR	-
P3	0-10	Ap	5YR 4/3	SCL	M	F,M	Gr	VH	FI	Gradual
	10-19	AB	5YR 3/3	SC	M	F,M	Sbk	VH	FR	Clear
	19-68	Bw1	10R 5/5	SC	M	F,M	Sbk	VH	FR	Gradual
	68-106	Bw2	2.5YR 4/4	SC	M	M	Sbk	H	VFR	Gradual
	106-157+	BC	2.5YR 5/6	SC	W	M	Sbk	H	VFR	-
P4	0-14	A	7.5YR 3/4	SC	S	M	Gr, sbk	H	FI	Gradual
	14-34	AB	5YR 3/4	C	M	VF	Sbk	SH	FR	Gradual
	34-78	BA	5YR 5/5	C	M	VF	Sbk	SH	VFR	Diffuse
	78-153	Bo	5YR 4/4	C	M	VF	Sbk	SH	VFR	Clear
	153-190	2Bw	10R 4/4	SCL	M	VF	Sbk	SH	VFR	Gradual
	190-200+	2BC	10R 5/6	SL	-	-	-	-	-	-
P5	0-17	Ap	5YR 4/3	SCL	S	M,C	Gr	H	FR	Gradual
	17-34	AB	5YR 4/3	C	S	F	Sbk	H	FR	Gradual
	34-116	Bt1	2.5YR 3.5/4	C	M	F	Sbk	H	VFR	Clear
	116-141	Bt2	10R 4/6	C	M	F	Sbk	H	VFR	Clear
	141-177+	BC	10R 4/6	C	M	F	Sbk	H	VFR	-
P6	0-27	Ap	10YR 4/2	SCL	M	C	Gr	H	FR	Gradual
	27-50	AB/BA	10YR 5/3	SCL	M	F	Sbk	H	FR	Clear
	50-88	Bw	10YR 4/6	SCL	M	F	Sbk	VH	FI	Clear
	88-140	BC	7.5YR 5/4	SCL	W	F	Sbk	H	FR	Clear
	140-180+	C	7.5YR 5/6	SL			Stratified sediment	H	FR	-

† Texture abbreviations: S = sand(y), C = clay, L = loam(y).

‡ Structure abbreviations: Gr = grade (W = weak, M = moderate, S = strong), Cl = class (VF = very fine, F = fine, M = medium, C = coarse), Sh = shape (Gr = granular, Sbk = subangular blocky).

§ Consistence abbreviations: Ad = air dry (H = hard, S = slightly, V = very), Fc = field capacity (FR = friable, FI = firm, V = very).

particle-size changes not attributable to stratigraphy of the gneiss, indicate that Profiles P2 and P3 formed in situ, from the saprolite residuum of biotite gneiss. Below them, on backslope positions, shallower Oxisols formed from the residuum of gneiss rock and related colluvium. They have a strong increase in clay content from the A to the AB horizon and a gradual distinctness of the horizon boundary (Tables 2 and 3). The subsurface horizons have reddish (5YR and 10R) hues, and lower CEC of clay than the Inceptisols on the MGS2.

On the footslope position, MGS3, a reddish (2.5YR and 10R in the Bt horizons) Ultisol formed, with chemical and mineralogical properties similar to the preceding Oxisols (Table 3). The illuviation process is shown in Profile P5, Bt1 horizon, by the gradual (from AB) distinctness of the horizon boundaries, the increase in clay content with depth (Table 3), and the common occurrence of argillans. Differences in slope gradient are probably responsible for the formation and preservation of an argillic horizon only in P5, as opposed to the incipient illuviation and predominance of oxic horizon properties in P4. According to Alexander (1995), the longer residence time of soil material on slopes with lesser gradient, due primarily to less erosion, allows more time for the translocation of clay downward to accumulate in argillic horizons (Profile P5). Thus, the frequency of argillic horizons is greatest on more gentle slopes.

Soil morphology and bulk density indicate the presence of dense horizons or firm layers in some of the profiles (Tables 2 and 3). Hard or very hard air-dry consistence (P6, Bw horizon) or greater bulk density than over- and underlying layers were observed mainly in the AB and upper B horizons of P5 and P6. A slightly greater bulk density was also observed in the Bo horizon of P4. The depth of occurrence does not indicate compaction due to agricultural practices. The presence of these dense or firm layers and their location in the transect may be related to the formation of a compressed layer by desiccation of the AB or BA transition horizons and of the upper B horizon, as proposed by Moniz and Buol (1982). There were no signs of chemical cementation in the examined horizons (Table 3).

The Inceptisol, P6, formed from fluvial deposits on the MGS4, shows the greatest base saturation (Table 3) compared with the other soils of the watershed. However, the clay CEC of the Bw horizon (13.7 cmol_c kg⁻¹, with correction for the CEC of organic matter, otherwise 18.4 cmol_c kg⁻¹) is within the range observed for low-activity clays (<24 cmol_c kg⁻¹), and the mineralogy shows only kaolinite and mica in the clay fraction, indicating neof ormation was not a major process. In Profile P6, the low amount of total Fe (29.4 g Fe_t kg⁻¹) stored in this low-lying position, the yellowish-brown (7.5YR and 10YR) colors, and the preservation of the easily weatherable primary minerals suggest the water table

Table 3. Some physical and chemical properties† of the soils.

Horizon	Clay	Bulk density	Total C	CEC	ECEC clay	BS	Si/Al	Fe _e	Fe _d	Fe _o
	g kg ⁻¹	Mg m ⁻³	g kg ⁻¹	cmol _c kg ⁻¹		%		g kg ⁻¹		
Profile P1										
Ap	490	1.26	20.1	16.0	10.1	22	1.75	37.8	16.6	1.2
AB	490	1.28	16.1	11.9	4.9	10	1.58	37.1	22.7	1.5
BA	540	1.31	12.1	9.9	3.1	7	1.68	39.2	20.6	1.4
Bo1	580	1.39	6.3	7.2	1.0	6	1.69	39.2	17.6	0.2
Bo2	600	1.19	3.4	4.9	0.8	8	1.71	41.3	21.7	0.0
Bo3	590	-	2.1	3.3	1.0	9	1.60	46.9	18.7	0.0
Profile P2										
A	350	1.69	18.5	13.2	9.1	15	1.86	37.1	23.9	2.5
Bw	340	1.41	7.9	6.1	3.2	14	1.80	46.2	32.4	1.5
BC	170	1.33	0.6	4.4	7.1	10	1.83	35.7	23.3	0.0
Profile P3										
Ap	300	1.48	17.8	15.3	10.3	16	1.94	32.2	22.0	1.6
AB	380	1.47	10.9	10.0	6.0	19	1.82	34.3	-	1.8
Bw1	380	1.52	6.4	7.6	5.5	16	1.87	37.8	25.2	1.5
Bw2	370	1.52	4.2	6.1	5.1	15	1.84	44.8	25.1	1.4
BC	360	1.43	4.1	3.9	5.8	31	1.77	39.2	24.8	1.3
Profile P4										
A	440	1.37	21.1	13.1	8.4	26	1.80	37.8	24.1	1.5
AB	580	1.28	13.0	11.2	4.7	15	1.74	47.6	25.5	1.1
BA	620	1.27	9.6	10.1	3.4	6	1.80	47.6	30.7	1.1
Bo	600	1.39	5.4	6.3	4.6	11	1.91	46.9	25.0	0.3
2Bw	270	-	2.5	3.7	8.3	48	1.73	44.1	24.7	1.1
Profile P5										
Ap	320	1.26	16.5	12.3	18.7	48	1.81	24.5	-	1.9
AB	490	1.45	13.8	9.1	6.7	29	1.75	35.7	25.4	1.8
Bt1	510	1.47	7.1	10.5	4.5	15	1.76	40.6	25.3	1.1
Bt2	600	1.37	2.2	6.0	3.8	25	1.94	48.3	31.6	0.4
BC	490	1.22	2.1	6.1	4.5	25	1.86	46.9	30.3	0.9
Profile P6										
Ap	230	1.45	11.4	9.0	27.8	71	2.28	21.7	14.9	3.4
AB/BA	310	1.45	5.7	7.2	14.8	64	2.16	27.3	18.3	2.5
Bw	310	1.56	3.2	5.7	11.6	63	2.16	29.4	18.8	2.0
BC	250	1.46	1.9	6.5	20.4	75	2.05	32.9	20.6	1.2
C	180	1.38	1.8	5.2	19.4	67	2.13	33.6	17.9	0.7

† CEC = cation-exchange capacity (sum of bases plus acidity); BS = base saturation (sum of bases \times 100/CEC); ECEC clay = effective CEC (sum of bases plus extracted Al³⁺) 100% clay; Fe_e = Fe extracted with H₂SO₄; Fe_d = Fe extracted with CBD; Fe_o = Fe extracted with oxalate.

was once shallow. The slightly greater Fe_o content and Fe_o/Fe_d ratio (Bw horizon, 2.0 g kg⁻¹ and 0.11, respectively) also suggest the occurrence of partially reductomorphic conditions in Profile P6 compared with the soils on the upper slope positions.

The leaching condition prevailing in the hillslope soils is reflected by their dystrophic or allic nature (here interpreted as having Al saturation \geq 50% in any diagnostic B horizon), as well as their low clay ECEC (Table 3). The CEC of clay (with organic C correction) from subsurface horizons ranges from 5.7 (P1) to 13.7 (P6) cmol_c kg⁻¹. Values for P4 (6.5 cmol_c kg⁻¹), on the back-slope position, are in conformity with the majority of Oxisols developed from granite-gneiss parent material in Rio de Janeiro State (Pereira, 1996). Effective CEC of the clay fraction was also calculated from the ECEC of the whole soil and the clay content, but without a subtracting factor for organic C contribution (footnote Table 3). Values of clay ECEC in the B horizon showed similar trends to the clay CEC, but with a wider range, from 0.8 (P1) to 11.6 (P6) cmol_c kg⁻¹.

The lowest value of Fe_d/clay is in the Oxisol (0.033) on the summit position and the greatest in the Inceptisols (0.095), indicating a modest contribution of Fe from the active weathering of primary minerals in the less developed soil profiles. The low and uniform Fe_d/Fe_e

and Fe_d/clay ratios with soil depth imply that Fe oxides are not acting as cementing agents at the transition and upper B horizons of Profiles P4, P5, and P6. Within the soil profiles, the greater Fe_o values (Table 3) are consistently found in the A horizons, where organic C is greatest.

Coarse and Fine Fraction Mineralogy

The sand fraction of all soils is predominantly of coarse size (2–0.2-mm diam.), and the proportion coarse/fine sand is fairly uniform. Skeleton grains (Table 4) are basically quartz, mostly of angular, subangular and subrounded, and spherical to subspherical shapes. Muscovite and altered biotite are relatively abundant in the fine sand fraction. Large concentrations of easily weatherable minerals (feldspars, biotite, etc.) were observed in the Inceptisols. Profiles P1 and P4, both Oxisols, show only traces of altered feldspars and mica. Profile P5, an Ultisol, has traces of feldspars and up to 1% of altered mica grains. Some resistant minerals, such as tourmaline, rutile-ilmenite, zircon, epidote, and sillimanite, are common to all soil profiles. They occur as traces or up to 1% in coarse and fine sand fractions. Fragments of charcoal and organic residues were found in the surface and upper B horizons of all soil profiles,

Table 4. Summary of mineralogy† of sand fraction in soil samples.

Horizon	Coarse sand (2–0.2 mm)				Fine sand (0.2–0.05 mm)			
	Qz	Mica	Fd	Cnct.	Qz	Mica	Fd	Cnct.
— % of grains‡ —								
Profile P1								
Ap	98	nd	tr	tr	97	tr	nd	tr
AB	98	tr	nd	1	98	tr	nd	nd
BA	99	nd	tr	tr	99	tr	tr	tr
Bo1	100	nd	nd	tr	100	tr	nd	tr
Bo2	100	nd	nd	tr	100	tr	nd	tr
Profile P2								
A	93	1	nd	3	73	10	nd	10
Bw	92	5	tr	3	55	30	tr	12
BC	92	3	nd	5	47	35	2	15
Profile P3								
Ap	90	2	1	4	78	7	2	8
AB	93	2	1	4	80	8	3	8
Bw1	95	1	tr	4	77	7	5	10
Bw2	90	3	1	5	76	10	3	10
BC	90	4	2	4	75	10	4	10
Profile P4								
A	90	2	tr	2	88	2	1	2
AB	97	tr	nd	1	97	tr	nd	1
BA	98	tr	tr	1	98	tr	tr	1
Bo	98	tr	tr	2	98	1	tr	tr
2Bw	85	5	2	8	70	15	tr	15
Profile P5								
Ap	93	1	tr	2	92	1	tr	2
AB	97	1	tr	1	95	1	tr	1
Bt1	98	1	tr	1	96	1	tr	1
Bt2	98	tr	tr	2	97	1	tr	1
BC	95	2	tr	2	91	5	tr	3
Profile P6								
Ap	90	tr	2	3	71	10	7	5
AB/BA	92	1	5	1	66	15	10	5
Bw	92	3	5	tr	50	35	10	4
BC	85	5	7	2	40	45	10	4

† Qz = quartz; Fd = feldspars; Cnct. = ferruginous concretions.

‡ nd = not detected; tr = traces, <1%.

in concentrations varying from traces to 7%, the highest values in the A (Ap) horizons.

According to x-ray diffraction analysis (Table 5), kaolinite is the dominant silicate clay mineral, and goethite occurs in small amounts as the dominant Fe oxide in all soils. In addition, the Oxisol on the summit has some peaks indicating traces of halloysite and of hydroxy-Al-interlayered vermiculite. The Inceptisols, formed from fresh rock (P2 and P3), have low amounts of mica. Profile P4, the Oxisol on the backslope, shows traces of halloysite and altered mica. Low amounts of illite, and traces of vermiculite, hydroxy-interlayered vermiculite, and gibbsite were detected in the Ultisol (P5) on the footslope. The Inceptisol (P6) formed from alluvium has very low amounts of goethite, and the greatest amounts of mica (biotite and illite) in the clay fraction.

Geomorphic Surfaces and Pedogenesis

Most models of soil genesis in the tropics (Moniz and Buol, 1982, and Curi and Franzmeier, 1984, in Brazil; Munnik et al., 1992, in South Africa; Peterschmitt et al., 1996 in South India) show a catenary differentiation of soils, with red Oxisols on ridge tops grading into red-yellowish Ultisols, and gray or mottled poorly drained, high base saturation soils toward the valley floor. Desilication and leaching are the major processes in the well-drained soils, combined with illuviation, dessication, and

lateral water flow on the slope soils, as opposed to resili-cation and accumulation of exchangeable cations in the valley bottom (Moniz and Buol, 1982). Normally, the hilltops are also characterized by a ferralitic domain with gibbsitic or hematitic Oxisols (Munnik et al., 1992; Peterschmitt et al., 1996). Analyses of the landscape and soil properties in the Caetés basin show that pedogenic intensity is strongly dependent on characteristics of the major geomorphic surfaces in the watershed (Fig. 1 and 2). They determine intensity of surface wash vs. solution loss, degree of weathering, depth of solum, illuviation process, and cation accumulation. The chemical removal process only declines when the water movement becomes restricted by the proximity of the groundwater table, as in MGS4, located at the valley bottom.

Generally, as pedogenesis progresses, these quantitative indexes change: (i) the solum depth becomes thicker; (ii) the silt/clay ratio decreases because clay-size minerals are mainly secondary minerals and many silt-size grains are primary minerals, so the silt/clay ratio reflects the ratio of primary to secondary minerals; (iii) the content of weatherable primary minerals decreases; (iv) the CEC/clay ratio decreases since the more highly weathered clay particles have little negative, and some positive, charges; (v) the Si/Al molar ratio decreases as primary and secondary minerals lose more Si than Al in weathering; (vi) the clay mineral suite reflects more weathering-resistant minerals, according to the sequence of Jackson and Sherman (1953) of soil development. Table 5 lists these index values according to the MGS described above.

The uppermost surface, MGS1, on the summit position, has a gently undulating surface (2% slope), and is freely drained. Surface MGS1 may not have developed from the underlying biotite gneiss, but it probably developed from the same kinds of rocks that were originally on a previous higher surface that is no longer present. On this geomorphic surface, solution loss reaches its maximum and the soils formed are intensively weathered. Profile P1 is clearly the most highly developed soil according to the index values (Table 5). The low values for many of the listed pedogenesis indices provide further evidence that the summit position, MGS1, is stable, and that it remains so until the retreating slope cuts through it. This supports the landscape evolution theories of King and Penck rather than that of Davis.

Surfaces MGS2 and MGS3 are intermediate in development according to the index values, and are younger than MGS1 (Daniels and Hammer, 1992). Surface MGS2 is a steeply sloping surface (20–35%) that cuts and descends from the summit. In the terminology of Ruhe (1960), it consists mainly of a backslope with smaller segments of shoulder. According to the processes postulated by King and Penck, it is identified as the retreating slope. Within MGS2, the amount of soil development increases downslope, as indicated by the decreasing amount of weatherable primary minerals, silt/clay ratio, and Fe ratios (Table 5) from P2 to P4. Surface wash processes predominate on the shoulder positions and the intensity of solution loss increases toward the backslope position.

Surface MGS3 consists of a set of rolling hills (5–15%

Table 5. Degree of pedogenesis according to quantitative indices calculated from properties of the major subsurface diagnostic horizons (average values).

Surfaces and profiles	Diagnostic subsurface horizons	Thickness	Silt/clay	wbpm, [†] fine sand	CEC/clay [‡]	Si/Al ratio	Fe _d /Fe _s [§]	Fe _a /Fe _s [§]	Fe _o /clay	Clay [¶] minerals (<2 μm)	Degree of pedogenesis
		cm		%	cmol kg ⁻¹						
MGS1 P1—Typic Hapludox	Bo1, Bo2, Bo3	161	0.04	traces	5.7	1.67	0.46	<0.01	0.033	K >> Go, HIV, Hly	High
MGS2 P2—Umbric Dystrochrept	Bw	34	0.59	30	7.5	1.80	0.70	0.05	0.095	K >> Mi	Low
P3—Umbric Dystrochrept	Bw1, Bw2	87	0.40	12–13	11.9	1.86	0.61	0.06	0.067	K >> Go, Mi	Low
P4—Typic Hapludox	Bo	75	0.08	traces to 1	6.5	1.91	0.53	0.01	0.042	K >> Go, II, Hly	Moderate
MGS3 P5—Typic Kandiudult	Bt1, Bt2	60	0.09	1	11.3	1.85	0.64	0.03	0.051	K >> Go, II, HIV, Gb	Moderate
MGS4 P6—Dystric Eutrochrept	Bw	38	0.52	45	13.7	2.16	0.64	0.11	0.061	K > Mi, II	Very low

[†] wbpm = weatherable primary minerals (mica and feldspars).

[‡] CEC/clay = [(CEC sum) - (4.5 × % organic C)] 100/% clay.

[§] Fe_d = H₂SO₄-extractable Fe; Fe_a = CBD-extractable Fe; Fe_o = oxalate-extractable Fe.

[¶] Relative amounts of minerals in the clay fraction: K = kaolinite; HIV = hydroxy interlayered vermiculite; Hly = halloysite; II = illite; Mi = mica (biotite); Go = goethite; Gb = gibbsite.

slopes) below the retreating slope. These hills have a smaller gradient and are less consistent in spatial distribution than the retreating slope. We believe that MGS3 formed in colluvium from the retreating slope, MGS2, so it is identified as the replacement slope according to Penck's ideas. Pedogenesis indices (Table 5) show values similar to the backslope profile on MGS2. Solution loss and translocation of colloids are the dominant process on MGS3.

In many places in the watershed, the surfaces of MGS2 and MGS3 blend smoothly into each other. This suggests that the retreating slope and the replacement slope could be the erosional and the depositional phase of the same surface, and they would be of about the same age. According to Schumm (1977), landscape evolution occurs as a result of periodic or episodic erosion, rather than at a uniform rate. If this theory applies to the Caetés watershed, MGS2 and MGS3 could consist of a set of much smaller geomorphic surfaces that vary considerably in age and in degree of soil development. Thus, the variability of P2, P3, P4, and P5 probably reflect differences in age of the geomorphic surfaces, but this relationship has not been elucidated because the geomorphic surfaces have not been mapped in detail.

Surface MGS4, on the toeslope, is the least developed surface according to all of the indices in Table 5. The surface is on alluvial deposits mixed with colluvium material, derived partly from local sediments that originated from drainageways in the hills and partly from the stream that occupies the valley. The soils on MGS4 have an accumulation of basic cations, probably a result of the weathering of feldspars and mica washed from unweathered gneiss on the head walls of the tributaries and leached from upper parts of the landscape.

CONCLUSIONS

Analyses of the landscape and soils in the Caetés basin show that pedogenic intensity is strongly dependent on the characteristics of the geomorphic surfaces. They de-

termine the intensity of surface wash vs. solution loss, degree of weathering, depth of solum, illuviation process, and cation accumulation on the valley floor. The degree of soil development, as represented by pedogenesis indices, is in accord with the landscape evolution theories of Penck and King. On the summit position, MGS1 is stable and a Typic Hapludox with the highest degree of pedogenesis formed. The upper part of the retreating slope, MGS2, bevels MGS1, and the material eroded from MGS2 moved downslope and formed a surface with lower gradient, MGS3. Dystrochrepts are on shoulder positions and shallow Hapludox are on backslope positions of the major geomorphic surface MGS2, and Kandiudults formed on footslopes, MGS3. Eutrochrepts are on the youngest surface, MGS4.

ACKNOWLEDGMENTS

We are grateful to Dr. Francesco Palmieri and other members of EMBRAPA/CNPS, UFRRJ, Departamento de Solos, and Purdue University, Agronomy Department and Atmospheric and Geological Sciences Department, for their technical assistance and scientific contributions. We are also very grateful to Dr. L. Darrell Norton, USDA-ARS National Soil Erosion Research Lab., and Dr. G. Steinhardt, Purdue University, for their valuable review and comments on the manuscript.

REFERENCES

- Alexander, E.B. 1995. Soil slope–depth relationships in the Klamath Mountains, California, and comparisons in central Nevada. *Soil Surv. Horiz.* 36:94–103.
- Bigarella, J.J., M.R. Mousinho, and J.X. Silva. 1965a. Considerações a respeito da evolução das vertentes. *Bol. Parana. Geogr.* 16–17:85–116.
- Bigarella, J.J., M.R. Mousinho, and J.X. Silva. 1965b. Processes and environments of the Brazilian Quaternary. p. 3–71. *In* Contrib. INQUA Congr. 7th, Symp. Cold Climate Process. Environ., Fairbanks, Alaska. April 1965. Universidade Federal do Paraná, Imprensa Universitária, Curitiba, Brazil.
- Carson, M.A., and M.J. Kirkby. 1972. *Hillslope form and process.* Cambridge Univ. Press, London.
- Curi, N., and D.P. Franzmeier. 1984. Soil genesis, morphology, and

- classification. Toposequence of Oxisols from the Central Plateau of Brazil. *Soil Sci. Soc. Am. J.* 48:341–346.
- Daniels, R.B., and R.D. Hammer. 1992. *Soil geomorphology*. John Wiley & Sons, New York.
- Departamento de Recursos Minerais. 1995. *Sinopse geológica do Estado do Rio de Janeiro: Texto explicativo do mapa geológico 1:40 000*. Secretaria de Estado do meio Ambiente, Niterói, RJ, Brazil.
- EMBRAPA/SNLCS. 1979. *Manual de métodos de análise de solo*. Empresa Brasileira de Pesquisa Agropecuária, Serviço Nacional de Levantamento e Conservação de Solos, Rio de Janeiro.
- EMBRAPA/SNLCS. 1988. *Sistema Brasileiro de classificação de solos. 3rd Approximation*. Empresa Brasileira de Pesquisa Agropecuária, Serviço Nacional de Levantamento e Conservação de Solos, Rio de Janeiro.
- Jackson, M.L. 1969. *Soil chemical analysis — Advanced course*. 2nd ed. M.L. Jackson, Madison, WI.
- Jackson, M.L., and G.D. Sherman. 1953. Chemical weathering of minerals in soils. *Adv. Agron.* 5:219–318.
- Mehra, O.P., and M.L. Jackson. 1960. Iron oxide removal from soils and clays by a dithionite–citrate–bicarbonate system buffered with sodium bicarbonate. *Clays Clay Miner.* 7:317–327.
- Milne, G. 1936. Normal erosion as a factor in soil profile development. *Nature (London)* 138:548–549.
- Moniz, A.C., and S.W. Buol. 1982. Formation of an Oxisol–Ultisol transition in São Paulo, Brazil: I. Double-water flow model of soil development. *Soil Sci. Soc. Am. J.* 46:1228–1233.
- Munnik, M.C., E. Verster, and T.H. van Rooyen. 1992. Spatial pattern and variability of soil and hillslope properties in a granitic landscape. 2. Pretoria — Johannesburg area. *S. Afr. J. Plant Soil* 9:43–51.
- Pereira, M.G. 1996. *Formas de Fe, Al e Mn como índices de pedogênese e adsorção de fósforo em solos do Estado do Rio de Janeiro*. Ph.D. diss. UFRRJ, Depto. de Solos, Seropédica, RJ, Brazil.
- Peterschmitt, E., E. Fritsch, J.L. Rajot, and A.J. Herbillon. 1996. Yellowing, bleaching and ferritization processes in soil mantle of the Western Ghâts, South India. *Geoderma* 74:235–253.
- Ruhe, R.V. 1960. Elements of the landscape. p. 165–170. *In* F.A. Beren et al. (ed.) *Trans. Int. Congr. Soil Sci.* 7th, Madison, WI. 14–24 Aug. 1960. Elsevier, Amsterdam.
- Salamuni, R., and J.J. Bigarella. 1967. The pre-Gondwana basement. p. 3–24. *In* J.J. Bigarella et al. (ed.) *Problems in Brazilian Gondwana geology. I*. Int. Symp. on the Gondwana stratigraphy and palaeontology, Mar del Plata, Argentine. Oct. 1965. Universidade Federal do Paraná, Imprensa Universitária, Curitiba, Brazil.
- Schumm, S.A. 1977. *The fluvial system*. John Wiley & Sons, New York.
- Schwertmann, U. 1964. Differenzierung der eisenoxide des bodens durch extraktion mit ammoniumoxalate-losung. *Z. Pflanzenernaehr. Dung. Bodenkd.* 105:194–202.
- Soil Survey Staff. 1993. *Soil survey manual*. 2nd ed. USDA-SCS Agric. Handb. 18. U.S. Gov. Print. Office, Washington, DC.
- Soil Survey Staff. 1996. *Keys to soil taxonomy*. 7th ed. Soil Manage. Support Serv. Tech. Monogr. no. 19. Pochahontas Press, Blacksburg, VA.
- Van Wambeke, A. 1981. Calculated soil moisture and temperature regimes of South America. *Soil Manage. Support Serv. Tech. Monogr. no. 2*. U.S. Gov. Print. Office, Washington, DC.
- Winchell, A.N., and H. Winchell. 1951. *Elements of optical mineralogy*. 4th ed. John Wiley & Sons, New York.